STATISTICS, OPTIMIZATION AND INFORMATION COMPUTING
*Stat., Optim. Inf. Comput.*, Vol. **11**, January 2023, pp 2–21.
Published online in International Academic Press (www.IAPress.org)

# An accelerated alternating iterative algorithm for data completion problems connected with Helmholtz equation

Karzan A. Berdawood [1,2], Abdeljalil Nachaoui [2], Mourad Nachaoui [3,*]

[1]*Department of Mathematics, College of Science, Salahaddin University-Erbil, Iraq*
[2]*Laboratoire de Mathématiques Jean Leray, Nantes Université, France*
[3]*Equipe de Mathématiques et Intercations, Université Sultan Moulay Slimane, Béni-Mellal, Maroc*

**Abstract** This paper deals with an inverse problem governed by the Helmholtz equation. It consists in recovering lacking data on a part of the boundary based on the Cauchy data on the other part. We propose an optimal choice of the relaxation parameter calculated dynamically at each iteration. This choice of relaxation parameter ensures convergence without prior determination of the interval of the relaxation factor required in our previous work. The numerous numerical example shows that the number of iterations is drastically reduced and thus, our new relaxed algorithm guarantees the convergence for all wavenumber $k$ and gives an automatic acceleration without any intervention of the user.

**Keywords** Inverse Cauchy problem; Helmholtz equation; Relaxed iterative method; Dynamical relaxation; Numerical simulation.

**AMS 2010 subject classifications** 35R30, 35J05, 65N20

**DOI:** 10.19139/soic-2310-5070-1702

## 1. Introduction

The original linear mathematical formula of the Helmholtz equation reverts to the wave equation with time-independent vector fields [16, 34].This type of equation has many applications in various fields of physics, such as optics, acoustics, electrostatics and quantum mechanics. Moreover, solving Helmholtz boundary problem requires several information, geometry of the domain, initial and boundary conditions, properties for the materials, influential forces in the domain. Nevertheless, in many engineering and physical problems these parameters are unknown, inaccessible or not measured. Indeed, it is needful to identify some of these parameters. These kind of questions belong to a class of problems called inverse problems. There are considerable inverse problems that appear in enormous number of physical and engineering applications, the usage of these problems varies depending on the type of the boundary conditions (Dirichlet, Neumann or mixed boundary conditions). For instance, it used for locating small-size tumors in the body for the human [54], for the discovision of the exporter of acoustical noise and surface oscillation from the internal acoustical pressure [18, 19], for determining an acoustic cavities and the radiation area surrounding a source of radiation [53, 14], for identifying the weld pool in process of welding [11, 9] and so on. In practical situations due to either inaccessibility of geometry, some physical obstacles, the over-specified or under-specified data will be appear. In particular, for these kind of problems it is possible to measure both the trace of the solution and the normal component of the field on one part of the boundary of the domain, while no information is available on the another remaining part. Consequently, determining and handling

*Correspondence to: Mourad Nachaoui (Email: nachaoui@gmail.com). Equipe de Mathématiques et Intercations, Université Sultan Moulay Slimane, Béni-Mellal, Maroc.

ISSN 2310-5070 (online) ISSN 2311-004X (print)

the missing solution and its normal derivative on this remaining part of the boundary is required. These kind of the problems are called Cauchy problems and it's a classical type of inverse problems [21, 21, 49, 50]. In the sense of Hadamard [26] these problems are severe ill posed problems. This means that, it may suffer from lack at least one of these conditions, existence, uniqueness and stability for numerical solution. The existence of the solution for the ill-posed Cauchy problem is guaranteed, if the boundary conditions on accessible part satisfy compatibility condition [28] . While, the uniqueness of the this problem is ensured with no limitation [17], one has to be careful with the stability since small noise in the data can cause a large variation between the solution obtained by perturbed data and that corresponding to unperturbed data [27].

To overcome of the ill-posedness nature for the Cauchy problem several performing methods has been investigated. In the last decades, the most common used method between the authors was regularization technique introduced by Tikhonov and Lavrentèv [55, 41]. The basic concept of this method consists in transforming the initial problem to a well-posed one by adding a penalty term that rely on a regularization parameter [52, 51]. For extra knowledge, we also want to recall another more widespread method whose called quasi-reversibility, which is introduced by Lions and Latts [38, 40, 39] to solve the inverse Cauchy problem with elliptic operator. The basic idea of this method is to convert the initial problem in to a family of fourth-order well-posed problems which depends on a tiny parameter $\epsilon$. Some others methods are based on the use optimization tools [1, 12, 35]. The disadvantage for all previous methods goes back to need for prior information on the solution of the inverse Cauchy problem. In addition to the disruption of the original operator by adding a small parameter.

In last three decades, an alternating iterative algorithm was introduced by the Kozlov et al. [37] (KMF).The algorithm is based on splitting the original ill-posed boundary problem into the sequence of well-posed boundary problems. The main advantages of this method consist in: firstly, the computational schemes can be implemented easily. Secondly, the schemes for the problems with linear and nonlinear operators are similar [47, 23, 22]. Finally, it does not require any chosen regularization parameter as in the previous methods. In [37, 36], the authors showed theoretical results concerning convergence, stability and regularization properties of the KMF algorithm but they gave no numerical results. Jourhmane and Nachaoui [32] used this technique for study inverse problem in bio-electric field and they found that this method produces a slowly convergent. Later, Nachaoui and his co-authors solved this problem by introducing a relaxation parameter [33], for which they show the existence of a convergence interval and another of convergence acceleration [48]. These two intervals are determined from the problem data.

For the Cauchy problem associated with Helmholtz equation, several papers have indicated that the KMF algorithm loses its efficiency especially for large enough wavenumbers. Either it does not converge or the convergence becomes so slow that it can be assimilated to non-convergence [4, 7, 8].

In order to be able to solve these problems which cannot be treated by this algorithm, we have suggested in previous works [4] an iterative relaxation method that can circumvent these obstacles. As for the Poisson equation [48], convergence and acceleration intervals, depending on the data of the problem, have been found. Unfortunately, in some cases, the convergence interval becomes very small, making it difficult to define that of the acceleration in a clear way and the choice of an optimal parameter becomes a complex procedure. Indeed for very close relaxation parameters one can pass from an acceptable number of iterations to a very slow convergence. In order to avoid these disadvantages, we propose in this paper a new iterative alternate relaxation method allowing a certain comfort for the user As the method uses an adaptive dynamical relaxation parameter which is updated through each iteration operation, we are exempt from the search for the optimal relaxation parameter. This method guarantees convergence without restriction on the wavenumber $k$ and drastically accelerates convergence.

We demonstrate that this dynamic relaxation parameter is an optimal parameter at each iteration, i.e. it allows the stopping criterion to decrease. This shows that it ensures convergence without worrying about finding the convergence interval. Moreover, this character of optimality makes it possible to obtain a formula allowing its evaluation at each iteration. This endows the method with a character of automaticity and makes it very attractive.

Note that the idea has been used in [5] for the Cauchy problem governed by the modified Helmholtz equation. But the dynamic relaxation parameter is used as a convergence accelerator of the KMF algorithm which is convergent in this case. Its use here makes it possible to obtain a convergent and very fast method not depending on any particular parameter in the case where the KMF algorithm does not work. It also makes it possible to quickly

obtain a solution in the case where the relaxation parameter, in the method proposed by the authors previously, becomes very complicated to find. It therefore presents a very good alternative to the algorithms used in [5, 7, 8].

The framework of the paper is as follows: in Section 2, we take a look at for Mathematical formulation for Cauchy problem. We devoted Section 3 for the classical iterative method(KMF). We propose in Section 4, two relaxed algorithms based on fixed and automatics parameter. In Section 5, the numerical results obtained by using the finite element method are given. For the numerical experiments, we include three different geometry namely the rectangle, circle and annulus with several choice of wave number $k$.

## 2. Mathematical formulation

Let $\Omega$ be a bounded domain in $\mathbb{R}^n$, $n \geq 2$ with a Lipschitz boundary $\Gamma$. Let $\Gamma = \Gamma_0 \cup \Gamma_1 \cup \Gamma_2$ where $\Gamma_i \neq \emptyset, i = 0, 1$, and $\Gamma_i \cap \Gamma_j = \emptyset$ for $i \neq j$. If $\Gamma_2 \neq \emptyset$ then either Dirichlet, Neumann or Robin condition may be specified on this part of boundary. In the following, suppose that $\Gamma_2 \neq \emptyset$, denote by $\nu$ the outward unite normal to the boundary $\Omega$ and consider the following Cauchy problem for the Helmholtz equation:

$$\Delta u + k^2 u = 0, \quad \text{in } \Omega, \tag{1}$$
$$u = f_1, \quad \text{on } \Gamma_1, \tag{2}$$
$$\partial_\nu u = f_2, \quad \text{on } \Gamma_1, \tag{3}$$
$$u = g_1, \quad \text{on } \Gamma_2, \tag{4}$$

where the positive real constant $k$ is the wave number and $\partial_\nu$ denotes the outward normal derivative of $u$. The function $g_1$ is the given data on $\Gamma_2$, the functions $f_1$ and $f_2$ are the known Cauchy data on $\Gamma_1$ and for $\Gamma_0$ all information are missing and must be determined. Thus problem Eqs. (1) to (4) is an inverse Cauchy problems with over-specified boundary $\Gamma_1$.

In the following sections we present the idea on which the KMF algorithm is based. then we present its modification as it was introduced in [4] and we finish by presenting our algorithm. the objective is to compare between these three algorithms and understand the contribution that our algorithm brings.

## 3. The alternating iterative method

The alternating method is an iterative procedure for solving inverse Cauchy problems. It works by repeatedly changing boundary Dirichlet-Neumann conditions until a stopping criterion is satisfied. This algorithm is based on solving at each step two well-posed problems for the original differential equation. The regularizing character of the alternating algorithm is only guaranteed by a suitable choice of boundary Dirichlet-Neumann conditions at each iteration on the under-specified boundary. In [36] the authors introduced this method as a tool to solve the Cauchy problem for elliptic equations. They proved the convergence of the algorithm and showed its regularizing properties. But no numerical result was given. Subsequently, this algorithm was implemented numerically in [31] and improved by the authors of [32, 33].

Many studies were then conducted using these methods to solve ill-posed problems arising from partial differential equations; See [2, 6, 10, 13, 15, 20, 22, 5, 46, 45]. To describe this procedure for solving the problem Eqs. (1) to (4), we start by writing the following two auxiliary problems to be solved at each iteration

$$\Delta u + k^2 u = 0, \quad \text{in } \Omega, \tag{5}$$
$$u = v, \quad \text{on } \Gamma_0, \tag{6}$$
$$\partial_\nu u = f_2, \quad \text{on } \Gamma_1, \tag{7}$$
$$u = g_1, \quad \text{on } \Gamma_2, \tag{8}$$

and

$$\Delta u + k^2 u = 0, \quad \text{in } \Omega, \tag{9}$$
$$\partial_\nu u = \eta, \quad \text{on } \Gamma_0, \tag{10}$$
$$u = f_1, \quad \text{on } \Gamma_1, \tag{11}$$
$$u = g_1, \quad \text{on } \Gamma_2, \tag{12}$$

where $f_1$ and $f_2$ are the Cauchy data given in Eqs. (3) to (4), hile $v$ and $\eta$ are two functions that must be updated at each iteration

Problems Eqs. (5) to (7) and Eqs. (9) to (11) must be solved alternately until the specified stopping criterion is satisfied and this action gives rise to classical KMF iterative algorithm that we describe in the following form:

**Algorithm 1:** Classic Alternating Approach KMF

1: $m \leftarrow 0$, select an initial estimate $v = v^0$, then,
2: Find $u^{(2m)}$ by solving the problem Eqs. (5) to (8).
3: Having computing $\eta = \partial_\nu u^{(2m)}$, find $u^{(2m+1)}$ by solving the problem Eqs. (9) to (12).
4: If $|| u^{(2m+2)} - u^{(2m)} ||_{L^2(\Gamma_0)} < \varepsilon$ then stop.
5: Else, $m \leftarrow m + 1$, then,
6: Compute $v = v^{(m)} = u^{(2m-1)} |_{\Gamma_0}$ and go to step 2.

The study of Cauchy problem associated to Helmholtz equation has been dealt with the KMF method by many authors, for instance see to [30, 43, 42, 7, 29]. Some of these authors commented that this algorithm is not convergent in many cases, especially when the wave number $k$ is large. It has also been reported that even when convergence is assured, it is achieved at a very high cost, namely a very large number of iterations. A first modification was done in [7, 8] where the authors proposed new modifications on the KMF algorithms through adding some regularization parameter resulting from introducing an artificial boundary to original problem. This approach has a drawback, namely that the nature of the problem is modified with a complexity of application. We then proposed alternate relaxation algorithms to solve the Cauchy Eqs. (1) to (4) problem, without any modification of the original domain of the problem and keeping the same principle of the KMF method but which circumvent the difficulties that she generates [4, 3].

## 4. The modified alternating iterative algorithm

The principal idea of the relaxation algorithm was initially introduced in [31] to solve the Cauchy problem of the Poisson equation. The convergence of the relaxation alternating iterative method has been demonstrated in [33]. This modification of the algorithm goes back in to increase the rate convergence for classic alternating algorithm KMF. This relaxation alternating algorithm was implemented and investigated for solving inverse Cauchy problem arising in many applications [24, 20, 44, 43, 10]. Hereafter, we will describe this algorithm to solve Cauchy Helmholtz problem. Particularly, in this study we will describe two relaxation algorithms.

### *4.1. The alternating relaxed algorithm with fixed factor*

The fixed relaxation algorithm as it was proposed in our previous work [4, 3] to solve the Cauchy problem for Helmholtz equation Eqs. (1) to (4) is summarized as follows.

**Algorithm 2:** Fixed relaxed alternating (FRA) approach

1: For $m \leftarrow 0$, specify an initial estimate $v = v^0$ of $u\mid_{\Gamma_0}$, and a relaxation parameter $0 < \theta < 2$, then,
2: Find $u^{(2m)}$ by solving the well posed problem Eqs. (5) to (8), with $v^{(0)} = v^0\mid_{\Gamma_0}$ and for $m > 0$,

$$v^{(m)} = \theta u^{(2m-1)}\mid_{\Gamma_0} +(1-\theta)v^{(m-1)}\mid_{\Gamma_0}. \tag{13}$$

3: Having construct $u^{(2m)}$ for $x \in \Omega$ and $\eta^{(m)} = \partial_\nu u^{(2m)}\mid_{\Gamma_0}$ the flux on $\Gamma_0$, find $u^{(2m+1)}$ by solving the following well posed problem Eqs. (9) to (12),
4: If $\| u^{(2m+2)} - u^{(2m)} \|_{L^2(\Gamma_0)} < \varepsilon$ then stop. Else, $m \leftarrow m+1$,, then, go to Step 2.

*Remark 1*
The classical KMF alternating algorithm can be recovered by taking the parameter $\theta = 1$ in Eq. (13). Thus, this algorithm is a generalization of the KMF algorithm.

### *4.2. An Alternating relaxed algorithm with dynamic factor*

The proposed technique of the dynamic relaxation algorithm is based on an automatic updating of the relaxation factor. Its strength is to find automatically and at each iteration the best relaxation parameter independently of the initial estimate. Thus dynamic relaxation, avoids the use of parameters or regularizations which must be selected by the user.This implicitly guarantees convergence for all values of $k$ and we will see through the numerical results that this method improves the convergence rate compared to the fixed relaxed alternating algorithm. We circumvented this constraint by looking for a parameter which depends on the iterations but which ensures a better decrease in the difference between the successive iterations.

The strategy for obtaining a dynamic relaxation parameter is as follows: We start from the updating of the boundary condition defined in (13), i.e. $v^{(m)} \in H^{1/2}|_{\Gamma_0}$ such that $v^{(0)} = v^0\mid_{\Gamma_0}$ and

$$v^{(m)} = \theta u^{(2m-1)}\mid_{\Gamma_0} +(1-\theta)v^{(m-1)}\mid_{\Gamma_0}. \tag{14}$$

For $m > 1$, we take $\theta = \theta^{(m)}$, where $\theta^{(m)}$ is unique real minimizing

$$\Psi(\theta) = \| v^{(m+1)} - v^{(m)} \|^2_{\Gamma_0}. \tag{15}$$

This ensures a reduction of the stopping criterion and therefore leads to a convergence of the sequence $u^{(m)}$.

From Eq. (14) we obtain

$$v^{(m+1)} - v^{(m)} = \theta\left(u^{(2m+1)}\mid_{\Gamma_0} - u^{(2m-1)}\mid_{\Gamma_0}\right) + (1-\theta)\left(v^{(m)} - v^{(m-1)}\right). \tag{16}$$

Now, using the fact that on the boundary $\Gamma_0$ we have $v^{(m)}$ given by $v^{(m)} = u^{(2m)}$ and $v^{(m-1)} = u^{(2(m-1))}$, see (6), we can rewrite (Eq. (16)) as

$$v^{(m+1)} - v^{(m)} = \theta\left(u^{(2m+1)}\mid_{\Gamma_0} - u^{(2m-1)}\mid_{\Gamma_0}\right) + (1-\theta)\left(u^{(2m)}\mid_{\Gamma_0} - u^{(2(m-1))}\mid_{\Gamma_0}\right). \tag{17}$$

Let

$$s^{(2m+1)} = u^{(2m+1)}\mid_{\Gamma_0} - u^{(2m-1)}\mid_{\Gamma_0},$$

and

$$s^{(2m)} = u^{(2m)}\mid_{\Gamma_0} - u^{(2(m-1))}\mid_{\Gamma_0},$$

then, the $\Psi$ function takes the form

$$\Psi(\theta) = || \, \theta s^{(2m+1)} - (1-\theta)s^{(2m)} \, ||^2_{\Gamma_0}, \tag{18}$$

or in a more expanded form:

$$\Psi(\theta) = \theta^2 \, || \, s^{(2m+1)} \, ||^2_{\Gamma_0} + 2\theta(1-\theta)\langle s^{(2m+1)}, s^{(2m)} \rangle + (1-\theta)^2 \, || \, s^{(2m)} \, ||^2_{\Gamma_0}, \tag{19}$$

where $\langle \cdot, \cdot \rangle$ is inner product in $L^2(\Gamma_0)$.

The function $\Psi(\theta)$ is minimized when $\frac{\partial \Psi}{\partial \theta} = 0$ and this is satisfied if

$$0 = \theta \, || \, s^{(2m+1)} \, ||^2_{\Gamma_0} + (1-2\theta)\langle s^{(2m+1)}, s^{(2m)} \rangle - (1-\theta) \, || \, s^{(2m)} \, ||^2_{\Gamma_0}, \tag{20}$$

what is ensured by the dynamic relaxation parameter $\theta = \theta^{(m)}$ given by:

$$\theta^{(m)} = \frac{\langle s^{(2m)}, s^{(2m)} - s^{(2m+1)} \rangle}{|| \, s^{(2m+1)} - s^{(2m)} \, ||^2_{\Gamma_0}}, \qquad \text{for } m > 1. \tag{21}$$

The introduction of this relaxation parameter in the (RFA) algorithm gives rise to our dynamic relaxation algorithm for solving the Cauchy problem Eqs. (1) to (4) which we summarize in **??** 3.

**Algorithm 3:** Dynamic relaxed Alternating (DRA) Approach

1: For $m \leftarrow 0$, specify an initial estimate $v = v^0$ of $u \, |_{\Gamma_0}$, and an initial factor $\theta^0$, then,
2: Find $u^{(2m)}$ by solving the well posed problem Eqs. (5) to (8), with $v^{(0)} = v^0 \, |_{\Gamma_0}$ and for $m > 0$,

$$v^{(m)} = \theta^m u^{(2m-1)} \, |_{\Gamma_0} \; + (1-\theta^m) v^{(m-1)} \, |_{\Gamma_0} \, . \tag{22}$$

3: Having construct $u^{(2m)}$ for $x \in \Omega$ and $\eta^{(m)} = \partial_\nu u^{(2m)} \, |_{\Gamma_0}$ the flux on $\Gamma_0$, find $u^{(2m+1)}$ by solving the following well posed problem Eqs. (9) to (12),
4: Compute $s^{(2m)} = u^{(2m)} \, |_{\Gamma_0} - u^{(2(m-1))} \, |_{\Gamma_0}$ and $s^{(2m+1)} = u^{(2m+1)} \, |_{\Gamma_0} - u^{(2(m-1))} \, |_{\Gamma_0}$ .
5: Compute $\theta^{(m)} = \frac{\langle s^{(2m)}, s^{(2m)} - s^{(2m+1)} \rangle}{||s^{(2m+1)} - s^{(2m)}||_{L^2(\Gamma_0)}}$.
6: If $|| \, u^{(2m+1)} - u^{(2m)} \, ||_{L^2(\Gamma_0)} < \varepsilon$, then stop. Else, $m \leftarrow m+1$, then, go to Step 2.

In order to compare the different algorithms presented in this paper, we will discuss the way to achieve convergence, namely the stopping criterion. It has been shown in several works, see for example [22, 45], that numerically the real error caused by the use of the relaxation alternation algorithm decreases very rapidly during the first iterations then this error grows to become stationary or continues to decrease but at a much slower rate. Thus, providing a stopping criterion allowing the execution of the algorithm to be terminated around the iteration where the algorithm becomes stationary would save time. we modify the usual stopping criterion to take account of this remark.

We are therefore going to compare the results obtained with two stopping criteria, the classic one and the one that we note modified criterion. The commonly used classical stopping criterion is the difference on $\Gamma_0$ between the solutions of two successive iterations $u^{(2m)}$ and $u^{(2m+2)}$ given by:

$$|| \, u^{(2m)} - u^{(2m+2)} \, ||_{L^2(\Gamma_0)} < \epsilon. \tag{23}$$

The stopping criterion (modified criterion) as it was suggested in [45] is based on the difference between the approximate solutions produced in two successive iterations, but this time these solutions are taken on the whole boundary $\Gamma$, i.e.

$$|| \, u^{(2m)} - u^{(2m+1)} \, ||_{L^2(\Gamma)} < \epsilon. \tag{24}$$

## 5. Numerical experiments

In this section, we present several numerical experiments with different given data. In order to solve the two well-posed boundary values problems that appear through all the iterative alternating procedures, we choose the finite element method which is more suitable for the study domain with complicated geometry.

We check also the numerical convergence with respect to concerning the nodes number on the boundary of the domain and we sudy the influence of fixed and dynamic relaxation parameters on the convergence and its speed.

We use the two stopping criteria described above, in order to prove the efficiency of the modified stopping criterion. We will subsequently adopt this last criterion for the rest of the experiments.

### *5.1. Example 1*

We consider $\Omega = ]0,1[\times]0,b[$ with $b > 0$. We shall solve the following Cauchy problem for Helmholtz equation

$$\Delta u + k^2 u = 0, \quad \text{in} \quad ]0,1[\times]0,b[, \tag{25}$$

$$u(x,0) = f_1, \quad \text{on } 0 \le x \le 1, \tag{26}$$

$$\partial_y u(x,0) = f_2, \quad \text{on } 0 \le x \le 1, \tag{27}$$

$$u(0,y) = u(1,y) = 0, \quad \text{on } 0 \le y \le b. \tag{28}$$

We take for more details $\Gamma_1 = ]0,1[\times\{0\}$, $\Gamma_0 = ]0,1[\times\{b\}$ and $\Gamma_2 = \{0\}\times]0,b[\cup\{1\}\times]0,b[$. For the numerical computations, we particularly choose $b = 0.2$ and select the boundary data $f_1(x) = u(x,0)$ on $\Gamma_1$ as

$$u(x,0) = \left(3\sin(\pi x) + \frac{\sin(3\pi x)}{19} + 9\exp(-30(x-b)^2\right) x^2(1-x)^2. \tag{29}$$

The exact boundary data on $\Gamma_0$, used to test the performance of the algorithm, is given by

$$ue(x,b) = 2\left(8\sin(\pi x) + \frac{\sin(3\pi x)}{17} + 20\exp(-50(x-b)^2\right) x^2(1-x)^2. \tag{30}$$

Note that the exact solution $u$ is unknown, thus, we first construct it by solving the direct problem for the Helmholtz equation Eq. (25) with boundary data Eq. (28), Eq. (29) and Eq. (30).

*Remark 2*
Note that an appropriate initial estimate $u_0 \in H^{1/2}(\Gamma_0)$ for the different numerical algorithms described above, must respect the compatibility conditions [25].

We choose $u_0 = 0$ as an initial estimate which satisfies the compatibility condition at the corner $\bar{\Gamma}_0 \cap \bar{\Gamma}_2$ and continuity of the first derivative at the corner $\bar{\Gamma}_0 \cap \bar{\Gamma}_2$. Note that this initial estimate is very far from the exact solution on $\Gamma_0$ (see Fig. 1).

For the following numerical experiment study, we will investigate convergence with respect to the numbers of nodes $N$ on $\Gamma_0$ and $M$ on $\{0\}\times]0,b[$ using finite element discretization. In Fig. 2 and Fig. 3 we ploted the classic and modified stopping criterion in 23 and 24 respectively as a function of the number iterations $m$.

By taking respectively the number of nodes $N \in \{100, 200, 400\}$ and $M \in \{20, 40, 80\}$, we see that the DRA algorithm converges with respect to the step of discretization.

The approximate solution gets closer and closer to the exact solution when the number of nodes increases. This is illustrated in Fig. 4, in which we represent the evolution of the numerical solution obtained through increasing nodes number $N$ and $M$.

We notice from Fig. 2 that the classic stopping criterion has a strong oscillation. It is not completely stable and it does not follow the real error behavior on $\Gamma_0$ for both cases $k = \sqrt{15}$ and $k = \sqrt{52}$.

On the other hand, for both wave numbers, we can observe from Fig. 3 that the modified stopping criterion has some oscillations for some first iterations, but it becomes stationary afterward. For $k = \sqrt{15}$ and $k = \sqrt{52}$, we can conclude according to Fig. 3 and Fig. 4 that, despite some oscillations, the modified stopping criterion imitates the behavior of the real error on $\Gamma_0$.

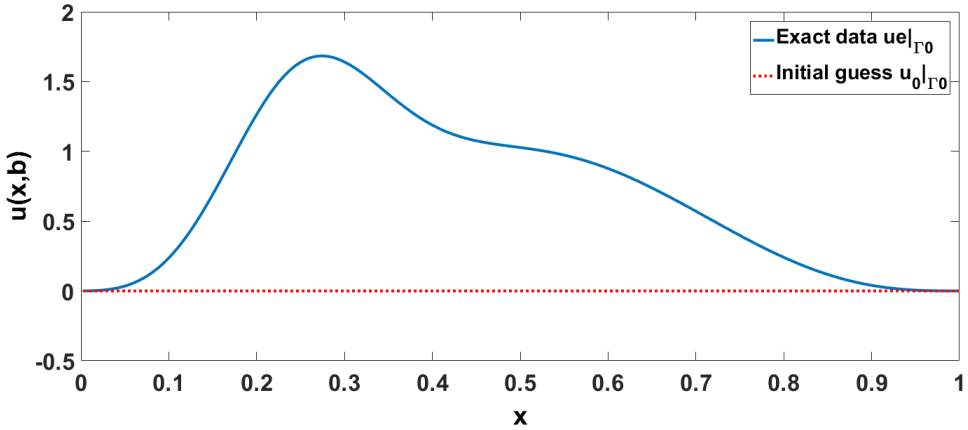


Figure 1. Initial estimate data and exact solution on $\Gamma_0$

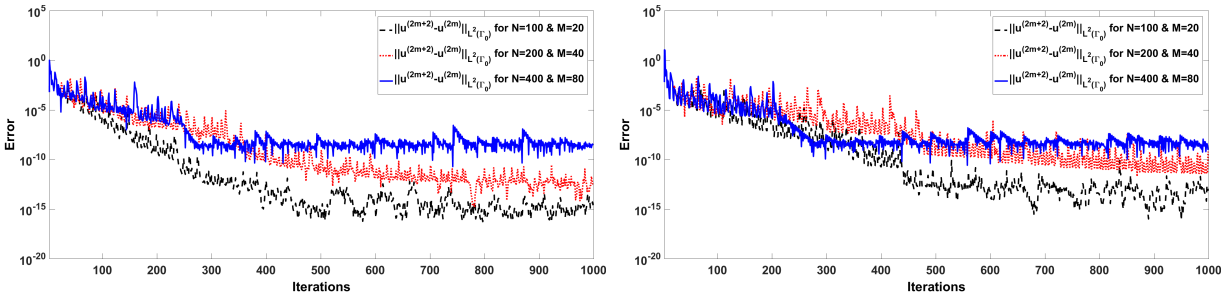


(a) (b)

Figure 2. Classical stopping criterion produced by the DRA algorithm, (a) $k = \sqrt{15}$ and (b) $k = \sqrt{52}$.

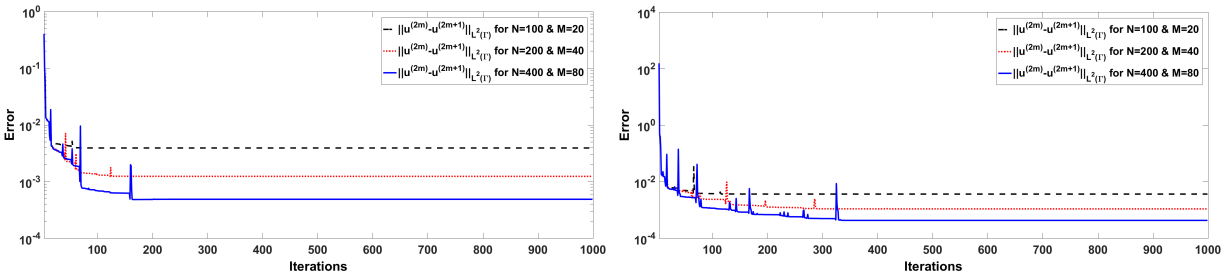


(a) (b)

Figure 3. Modified stopping criterion produced by the DRA algorithm, (a) $k = \sqrt{15}$ and (b) $k = \sqrt{52}$.

Therefore, by the indicator of stopping criterion, we can cancel all iterations which have no impact on decreasing real error.

We also notice that at some first iterations, the stopping criterion decreases very rapidly and it stops decreasing afterward, even though a large number of iterations are performed.

We observe from the representation of the relaxation parameter $\theta^m$ a strong oscillation corresponding to the automatic search for the most appropriate parameter at each iteration (see Fig. 6 for both cases $k = \sqrt{15}$ and $k = \sqrt{52}$).

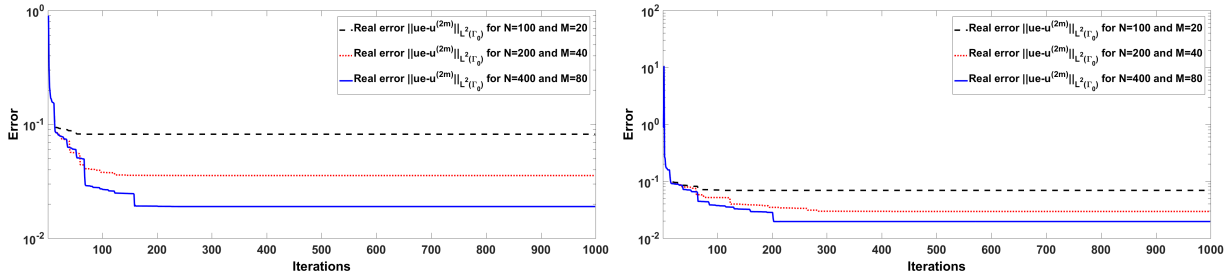


(a) (b)

Figure 4. Accuracy error as a function of the number of nodes for the DRA (a)$k = \sqrt{15}$, (b)$k = \sqrt{52}$.

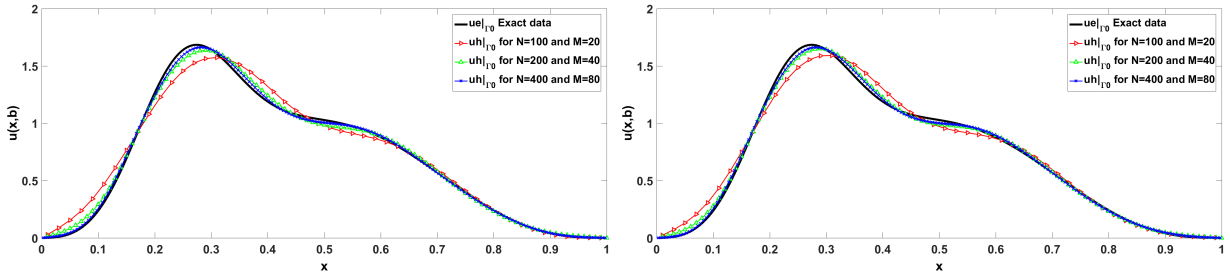


(a) (b)

Figure 5. Exact and reconstructed solutions on $\Gamma_0$, using DRA algorithm, $k = \sqrt{15}$ (a) , $k = \sqrt{52}$ (b).

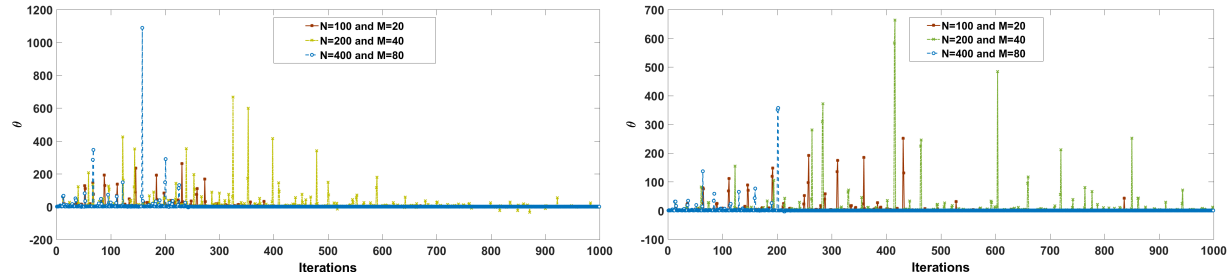


(a) (b)

Figure 6. Variation of $\theta^m$ for DRA algorithm, (a) $k = \sqrt{15}$, (b) $k = \sqrt{52}$.

This oscillation of the values of $\theta$ has direct impact on oscillation of the classic stopping criterion (see Fig. 2 for both $k = \sqrt{15}$ and $k = \sqrt{52}$ ) while it has not the same impact on modified stopping criterion (see Fig. 3 for both cases $k = \sqrt{15}$ and $k = \sqrt{52}$ ). Nevertheless, this strong or weak instability in the classic or modified stoping criterion with respect to different numbers $N$ and $M$ does not have any impacts on the behavior of the real error for both wave number $k = \sqrt{15}$ and $k = \sqrt{52}$ as it's shown in Fig. 3.

Always for cases $k = \sqrt{15}$ and $\sqrt{52}$, we observed through figures Fig. 3 and Fig. 5 that the accuracy errors decrease dramatically all at once in conjunction with the increase in value of dynamical $\theta$. We observe, from figures Fig. 8 and Fig. 10 corresponding respectively to $k = \sqrt{15}$ and $k = \sqrt{52}$, that the dynamic relaxation $\theta^m$ depends on $k$ and is not in $]0, 2[$ as required for the fixed parameter $\theta$. Both figures exhibit an oscillatory behavior of the relaxation factor $\theta^m$ which shows its dynamic variation in order to respond to the character of optimality at each iteration.

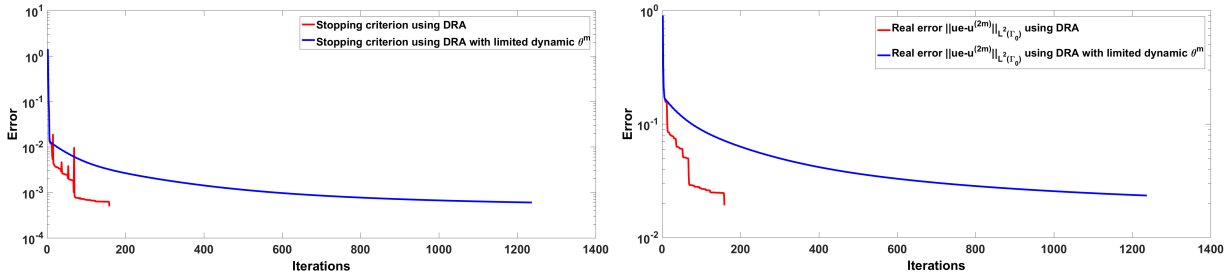


(a) (b)

Figure 7. DRA algorithm results for Example 1 with $k = \sqrt{15}$ , (a): Stopping criterion, (b) : Real error.

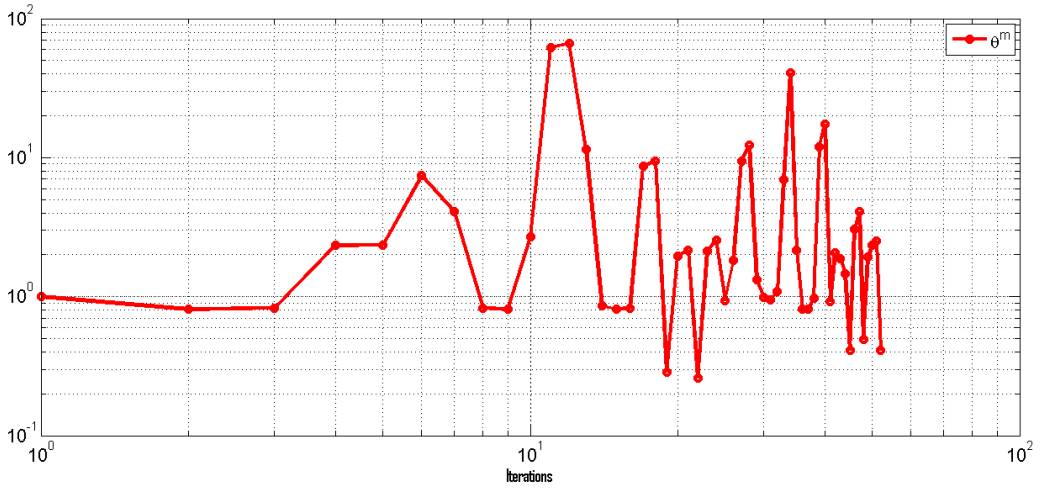


Figure 8. Evolution of $\theta^{(m)}$, using data on Example 1, for $k = \sqrt{15}$, with N=400 and M=80.

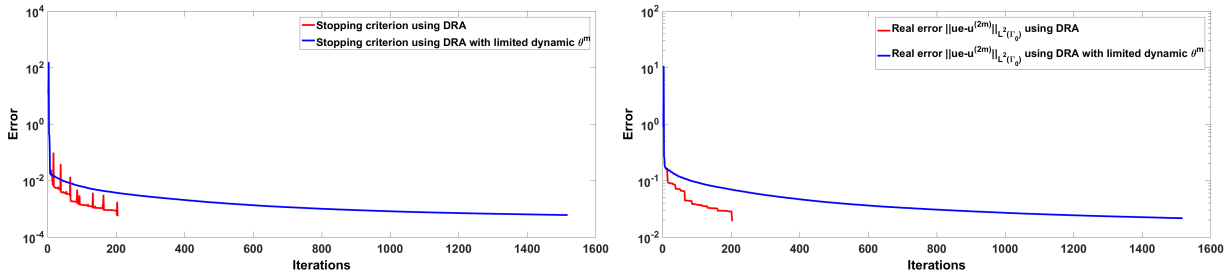


(a) (b)

Figure 9. DRA algorithm results for Example 1 with $k = \sqrt{52}$, (a) : Stopping criterion, (b): Real error.

We also used a projection of $\theta^m$ in the convergence interval $]0, 2[$ in order to respect the same conditions as for fixed $\theta$ in the RFA algorithm.

Through figures Fig. 7 and Fig. 9, we can see that the DRA algorithm converges in both cases $k = \sqrt{52}$ and $k = \sqrt{52}$ respectively. Furthermore, we observe from these figures that DRA remains faster than DRA with

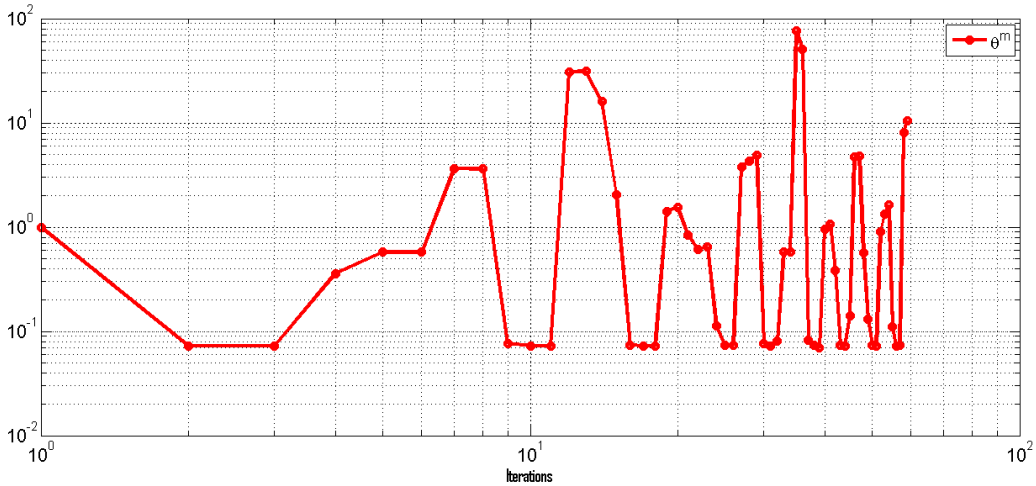


Figure 10. Evolution of $\theta^{(m)}$, using data on Example 1, for $k = \sqrt{52}$, with N=400 and M=80 .

projection of $\theta^m$, which proves that the character of optimality of the parameter obtained dynamically has its importance in the acceleration of convergence even if the $\theta^m$ are not in $]0, 2[$.

### *5.2. Numerical comparisons between the algorithms*

In order to show the performances of our dynamic relaxation algorithm DRA we compare its results with those produced by the fixed relaxation algorithm FRA knowing that the classical algorithm KMF corresponds to the case $\theta = 1$ in the FRA algorithm. We are interested in the comparison of the speed of the algorithms represented by the number of iterations and the quality of the approximate solution evaluated by the convergence error. These results are presented for different values of wavenumber $k$. The first results correspond to solving the Cauchy

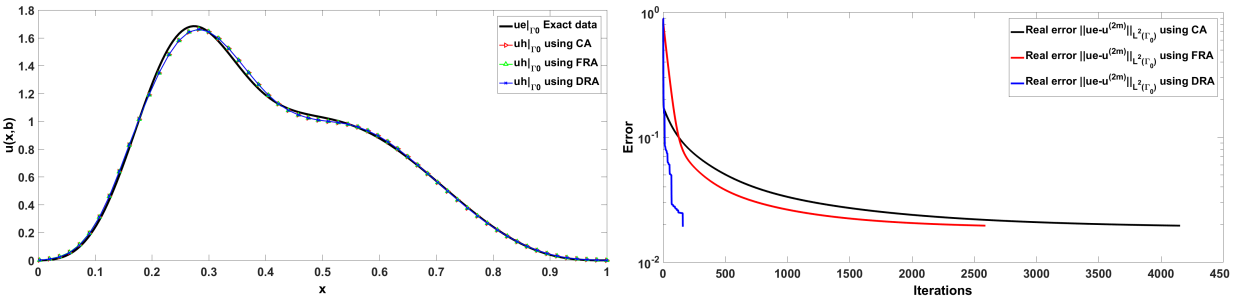


(a) (b)

Figure 11. Results for $k = \sqrt{15}$, (a): exact and reconstructed solutions on $\Gamma_0$ , (b): convergence history

problem Eq. (1)-Eq. (4) using data in Example 1 for three values of wave number $k = \{\sqrt{15}, \sqrt{52}, \sqrt{100}\}$. In all these examples, we take in the stopping criterion a tolerance $\epsilon = 10^{-4}$

It is clear from Fig. 11 that all algorithms give a good approximation with the same order of accuracy (for $k = \sqrt{15}$). We also observe that the DRA algorithm is faster than both KMF and FRA algorithms. More precisely, the DRA algorithm needed only $158$ iterations to reach the specified precision based on the proposed stopping criterion when the FRA algorithm required more than $2500$ and while it took $4000$ iterations to the KMF algorithm.

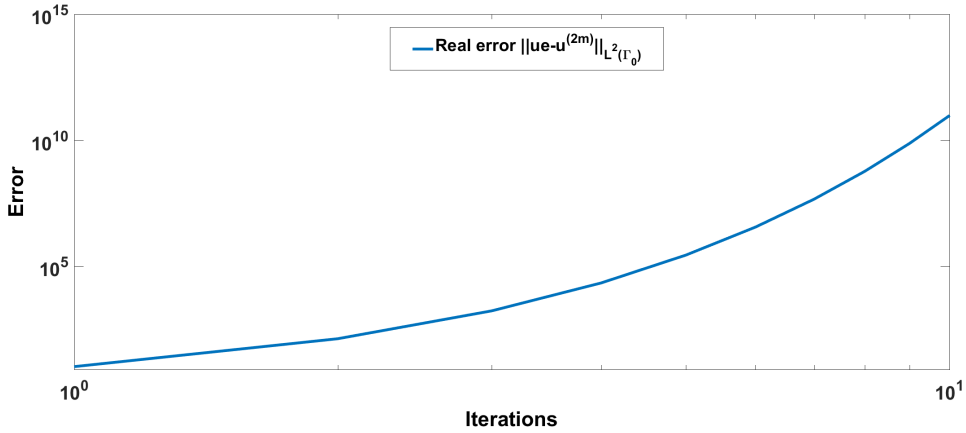


Figure 12. Divergence aspect of the KMF algorithm, using the data from Example 1 and $k = \sqrt{52}$.

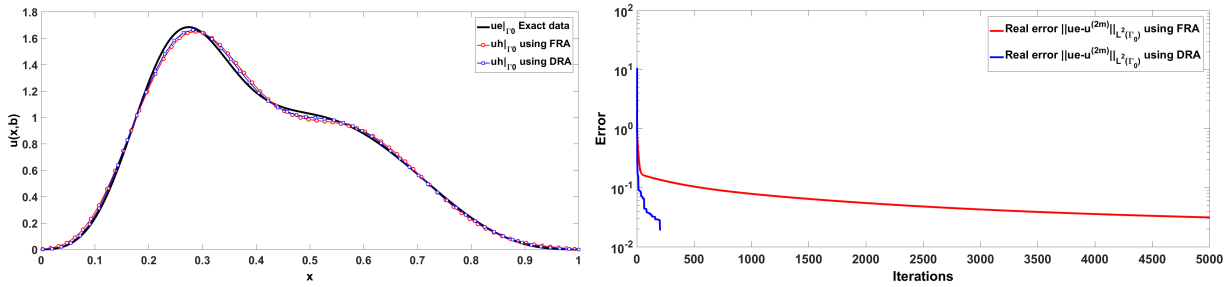


(a) (b)

Figure 13. Results for $k = \sqrt{52}$, (a): exact and reconstructed solutions on $\Gamma_0$ , (b): convergence history

In the Fig. 12 we display the divergence of the KMF algorithm for $k = \sqrt{52}$ by plotting the real error for 10 iterations. As we can see in Fig. 13 (a) the quality of the approximations obtained by both algorithms FRA and

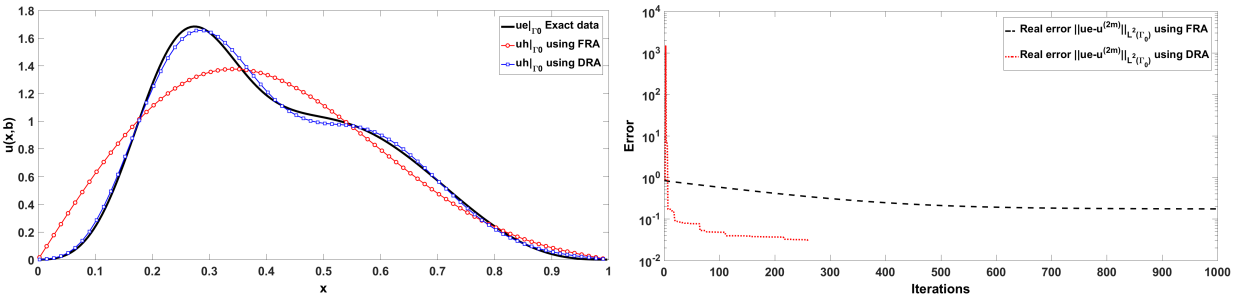


(a) (b)

Figure 14. Results for $k = \sqrt{100}$, (a): exact and reconstructed solutions on $\Gamma_0$ , (b): convergence history

DRA is good and the two approximate solutions are in perfect agreement with the exact solution. From Fig. 13 (b) it is clear that FRA algorithm with optimum $\theta$ is very slow, compared to DRA algorithm.Tthe first one needed more than 5000 iterations to reach the convergence when the second required just 202 iterations. We present in Fig. 14 the results corresponding to a large value of the wave number ($k = \sqrt{100}$). This is a case where the KMF algorithm

does not converge and for which the convergence interval required for the RFA algorithm is very small, which makes the isolation of an optimal parameter very complicated. This optimal parameter corresponds to $\theta = 0.001$. As can be seen in figure Fig. 14 (b), the convergence of the RFA algorithm is very slow. Figure Fig. 14 (a) shows that the quality of the approximate solution produced by this algorithm is poor, while the DRA algorithm produces a very good approximation for a reasonable number of iterations (260 iterations).

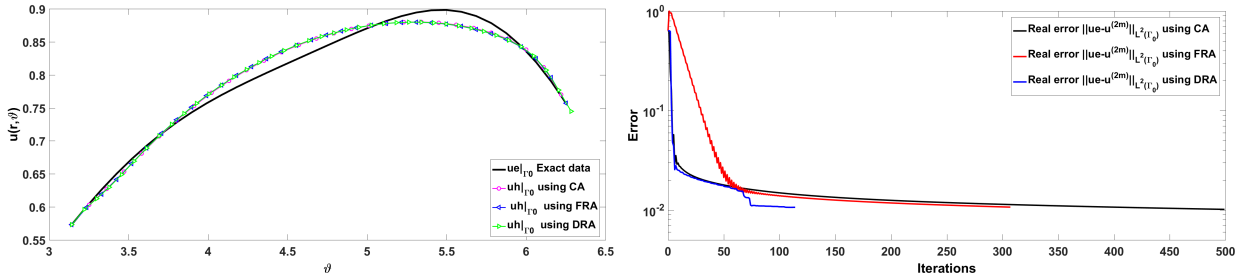


(a) (b)

Figure 15. Example 2 with $k = \sqrt{15}$, (a): exact and reconstructed solutions on $\Gamma_0$ , (b): convergence history

After having studied the quality of the algorithms proposed to solve the Cauchy problem Eq. (1)-Eq. (2) in the domain of the rectangle, we applied, in the second part of the numerical experiments, all the previous algorithms to this problem inverse with the data of example 1, posed in a disc. The finite element discretization is done for a fixed number of nodes equal to 200. The wavenumbers considered are $k = \sqrt{15}$ and $k = \sqrt{52}$. We only present results corresponding to the data of example 1, but other similar results were obtained for the other two examples. We present a numerical comparison between all the algorithms based on the accuracy and the computational cost. This shows the superiority of the DRA algorithm over the two algorithms.

### *5.3. Example 2*

Consider the Cauchy problem in a circular domain $\Omega = \{(x, y) \in \mathbb{R}^2 \ / \ x^2 + y^2 < r^2\}$. Suppose that the boundary $\partial\Omega := \Gamma_1 \cup \Gamma_0$, with

$$\Gamma_1 = \{(x, y) \in \partial\Omega \ / \ 0 < \vartheta(x, y) < \Theta\}, \ and \ \Gamma_0 = \{(x, y) \in \partial\Omega \ / \ \Theta < \vartheta(x, y) < 2\pi\},$$

where $\vartheta(x, y)$ is the polar angle of $(x, y)$ and $\Theta$ is a given angle in $]0, 2\pi[$. In this example we consider that $\Gamma_2 = \emptyset$.

For numerical test, we select the radius $r = 0.2$ and $\Theta = \pi$. After solving numerically the direct Helmholtz equation problem with Dirichlet data

$$f_1 = \sin(x + 1)\cosh(\sqrt{1 - k^2}(y + 2))$$

on the entire boundary $\Gamma$, the obtained solution is denoted $ue$. We calculate the normal derivative of this solution on $\Gamma_1$, which we denote $f_2$ and then reconstruct the trace of $ue$ on $\Gamma_0$ as a solution of the Cauchy problem with data $f_1$ and $f_2$.

It can be seen from Fig. 15 , that here also all algorithms give a good approximation with the same order of accuracy (for $k = \sqrt{15}$). One can also observe that the number of iterations is reduced form 500 iterations for KMF algorithm (130 for RFA) into 113 iterations for DRA algorithm which confirm again its superiority over the two algorithms.

Here too, we observe (see Fig. 16) that for a large wave number $k = \sqrt{52}$ the KMF algorithm diverges, while the FRA algorithm with the optimal parameter $\theta = 0.25$ and DRA algorithm converge with good precision. We also note that the DRA algorithm is much faster than the FRA algorithm. The first requires 306 iterations to reach the convergence while more than 1000 iterations are necessary for the second, see Fig. 17.

For the next part, as in the previous Examples, we investigated the comparison between algorithms based on on the speed of convergence and the precision of the produced numerical solutions using different values of the

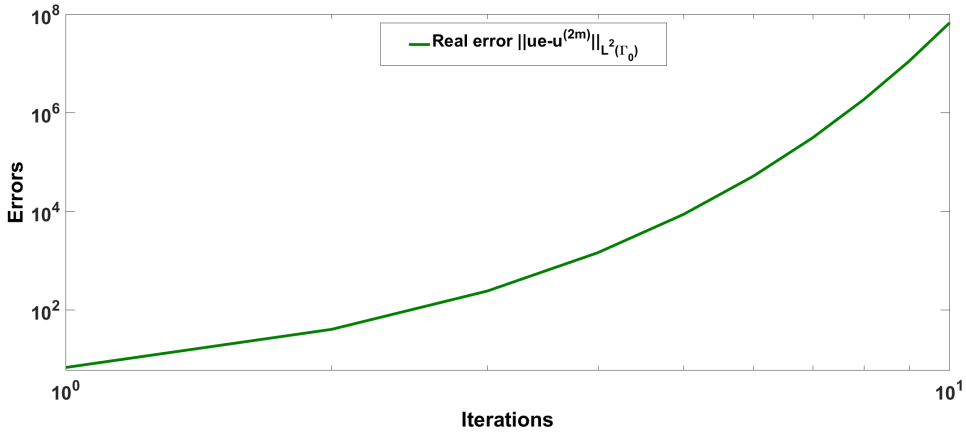


Figure 16. Divergence aspect of the KMF algorithm, using the data from Example 2 and $k = \sqrt{52}$.

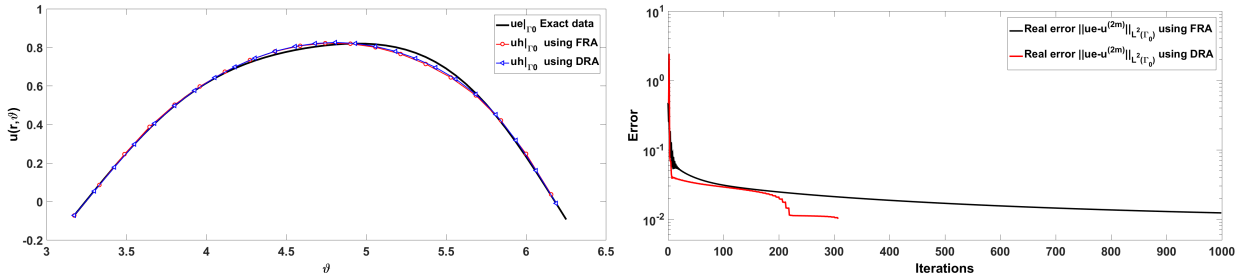


(a) (b)

Figure 17. Example 2 with $k = \sqrt{52}$, (a): exact and reconstructed solutions on $\Gamma_0$ , (b): convergence history

wavenumber $k$. The domain being the annular domain with the same conditions as for the previous numerical tests, but this time on example 3.

### *5.4. Example 3*

Consider the Cauchy problem on the annular domain, defined by the circles of radii $r_0 = 0.75$ and $r_1 = 1$, $\Omega = \{(x, y) \in \mathbb{R}^2 \ / \ r_0^2 < x^2 + y^2 < r_1^2\}$. The boundary is assumed to be composed of two part $\partial\Omega := \Gamma_1 \cup \Gamma_2$,

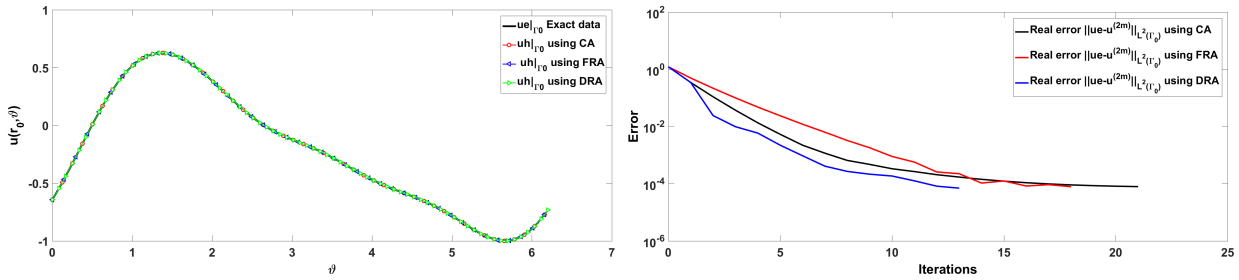


(a) (b)

Figure 18. Example 3 with $k = \sqrt{5}$, (a): exact and reconstructed solutions on $\Gamma_0$ , (b): convergence history.

with

$$\Gamma_1 = \{(x,y) \in \partial\Omega \ / \ x^2 + y^2 = r_0^2\}, \quad \Gamma_2 = \{(x,y) \in \partial\Omega \ / \ x^2 + y^2 = r_1^2\}.$$

All data for this problem are taken as in Example 2.

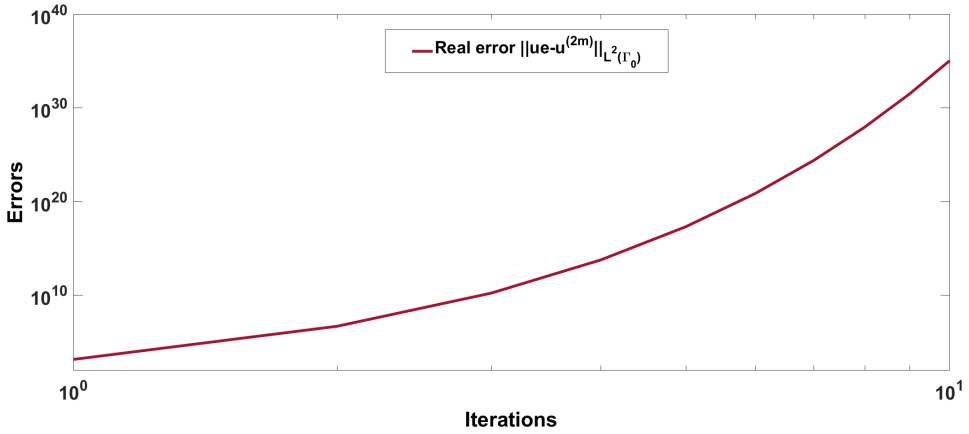


Figure 19. Divergence aspect of the KMF algorithm, using the data from Example 3 and $k = \sqrt{35}$.

First of all, in the case of the wavenumber $k = \sqrt{5}$, all algorithms are convergent, but the DRA algorithm is much faster see Fig. 18.

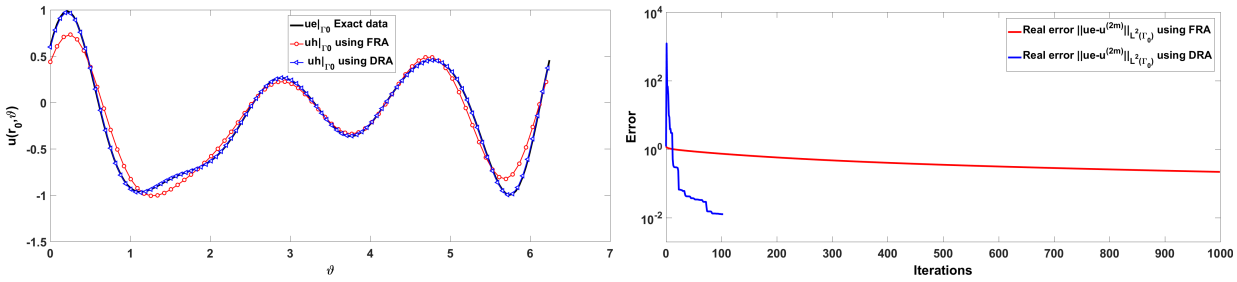


(a) (b)

Figure 20. Example 3 with $k = \sqrt{35}$, (a): exact and reconstructed solutions on $\Gamma_0$ , (b): convergence history.

For $k = \sqrt{35}$, the FRA algorithm with the optimum $\theta = 0.0005$ converges slowly (after 1,000 iterations) with low precision while the DRA algorithm, just after 103 iterations, achieved good accuracy. This is again explained by the convergence interval, which is very small and induces a low optimal value $\theta$ for the RFA algorithm see Fig. 20. Note that here again the KMF algorithm diverges see Fig. 19.

Finally, in the case where $k = \sqrt{52}$, the optimal value of $\theta$ allowing the best acceleration for the fixed relaxation algorithm (FRA) becomes close to zero, and consequently, its effect on convergence is negligible. While, the DRA algorithm shows its efficiency whether at the level of the speed of convergence or at the level of the quality of the numerical solution Fig. 21 .

### *5.5. Impact of the inaccessible boundary part on the convergence*

In this section, We seek to clarify the impact of increasing or decreasing length scale for inaccessible boundary ($\Gamma_0$) on the convergence and the approximation accuracy obtained by the DRA algorithm using data on Examples 2 and 3.

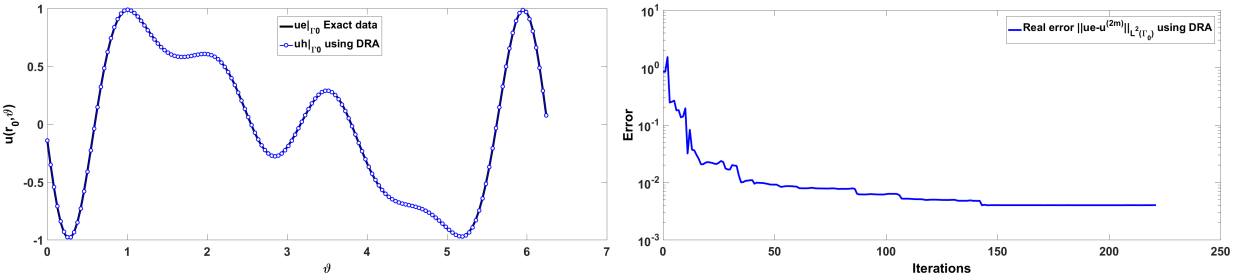


(a) (b)

Figure 21. DRA results for data in Example 3 and $k = \sqrt{52}$, (a): exact and reconstructed solutions on $\Gamma_0$, (b): convergence history.

| $mes(\Gamma_1) \geq mes(\Gamma_0)$ | | | |
|---|---|---|---|
| Angle | Node numbers on boundary | $\|u - ue\|_{L^2(\Omega)}$ | Number of iterations |
| $\Theta = \frac{3\pi}{2}$ | $N_{\|\Gamma_1} = 100$ and $M_{\|\Gamma_0} = 100$ | 0.00661591 | 91 |
| $\Theta = \pi$ | $N_{\|\Gamma_1} = 100$ and $M_{\|\Gamma_0} = 100$ | 0.0147404 | 186 |
| $mes(\Gamma_1) < mes(\Gamma_0)$ | | | |
| $\Theta = \frac{\pi}{2}$ | $N_{\|\Gamma_1} = 300$ and $M_{\|\Gamma_0} = 900$ | 0.0690919 | 388 |

Table 1. Example 2 with $k = \sqrt{52}$, illustration the effects the length of $\Gamma_0$

In fact, Table 1 presents the DRA algorithm results for the circular domain of example 2, with $k = \sqrt{52}$. The tolerance used for the modified stopping criterion is $\varepsilon = 10^{-04}$.

We observe from this table that in the case where $my(\Gamma_1) > my(\Gamma_0)$, the DRA algorithm converges quickly towards a very accurate solution. This quality of precision and speed deteriorates more and more as the length of the inaccessible part becomes greater and greater. But it still remains correct even when $mes(\Gamma_1)$ is three times smaller than $mes(\Gamma_0)$.

| $mes(\Gamma_1) > mes(\Gamma_0)$ | | | |
|---|---|---|---|
| Radius | Numbers of nodes | $\|u - ue\|_{L^2(\Omega)}$ | Number of iterations |
| $r_1 = 1.0, r_0 = 0.75$ | $N = 400, M = 300$ | 0.00540837 | 197 |
| $r_1 = 1.0, r_0 = 0.50$ | $N = 400, M = 200$ | 0.004019 | 221 |
| $r_1 = 1.0, r_0 = 0.25$ | $N = 400, M = 100$ | 0.00904027 | 216 |
| $mes(\Gamma_1) < mes(\Gamma_0)$ | | | |
| $r_1 = 0.75, r_0 = 1.0$ | $N = 300, M = 400$ | 0.0445471 | 264 |
| $r_1 = 0.50, r_0 = 1.0$ | $N = 750, M = 1500$ | 0.0975133 | 849 |

Table 2. Example 3 with $k = \sqrt{52}$, effects of the length of radius defining $\Gamma_0$

Table 2 illustrates the effect of the length of the radius of the inaccessible part in the case where the domain is an annular one. From this table we draw the same conclusions as those retained from the previous tables.

In accordance with the numerical comparisons previously studied, the superiority of our new DRA algorithm over the old ones in solving the inverse Cauchy problem has been proven. In the next section, we will therefore study the numerical stability only for the DRA algorithm applied to the various examples previously presented.

### *5.6. Numerical stability*

The solution of the inverse Cauchy problem not being continuously dependent on the data, which justifies that this problem is badly posed in the sense of Hadamard [26], without regularizing character, a method such as the one we have developed would not be relevant. We therefore present a study on the numerical stability of this algorithm in order to show its regularizing character.

We limit ourselves to examining the numerical stability for the wavenumber $k = \sqrt{52}$, which is considered to be a rather high wavenumber. In order to simulate measurement errors, the Dirichlet and Neumann boundary conditions in Eq. (2)-Eq. (3) on $\Gamma_1$ are perturbed by adding noise to the Cauchy data, in the form

$$f_1^\delta = f_1 + \delta f_1, \qquad f_2^\delta = f_2 + \delta f_2, \tag{31}$$

where $\delta f_1 = f_1 * \delta * (2 * rand - 1)$ and $\delta f_2 = f_2 * \delta * (2 * rand - 1)$ are Gaussian noises with a mean zero, generated by an appropriate $rand$ function. While the $\delta$ is the level of the noise. The Cauchy problem in Eq. (1)-Eq. (4) with respect to noise data is described by

$$\Delta u^\delta + k^2 u^\delta = 0, \quad \text{in} \quad \Omega, \tag{32}$$

$$u^\delta(x,0) = f_1^\delta, \quad \text{on } \Gamma_1, \tag{33}$$

$$\partial_y u^\delta(x,0) = f_2^\delta, \quad \text{on } \Gamma_1, \tag{34}$$

$$u^\delta(0,y) = u^\delta(1,y) = 0, \quad \text{on } \Gamma_2. \tag{35}$$

Four different noise levels $\delta \in [2.5 * 10^{-2}, 2 * 10^{-1}]$ were used. A comparison of the exact solution $ue$ , the noiseless approximate solution and the one approximated with noise of order $\delta$, $u^\delta$ is discussed in the following.

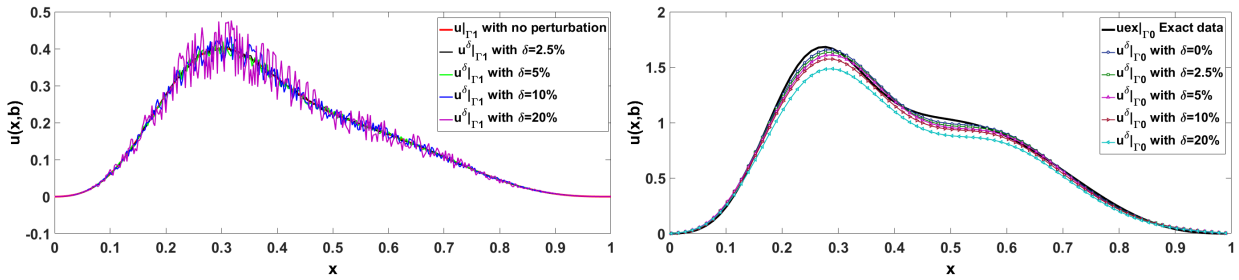


(a) (b)

Figure 22. Results for Example 1 with $k = \sqrt{52}$, (a): Noisy data on $\Gamma_1$ , (b): Corresponding solutions on $\Gamma_0$.

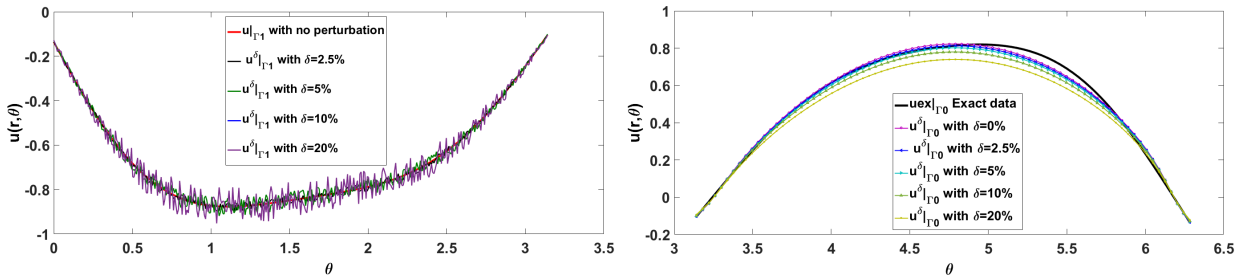


(a) (b)

Figure 23. Results for Example 2 with $k = \sqrt{52}$, (a): Noisy data on $\Gamma_1$ , (b): Corresponding solutions on $\Gamma_0$.

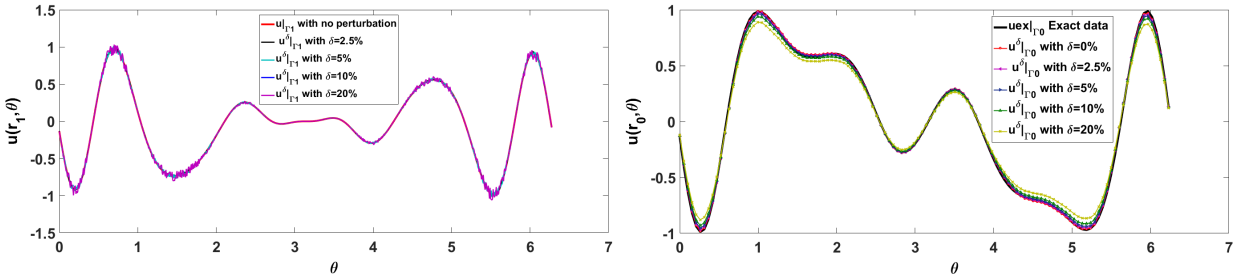


(a) (b)

Figure 24. Results for Example 3 with $k = \sqrt{52}$, (a): Noisy data on $\Gamma_1$ , (b): Corresponding solutions on $\Gamma_0$.

As can be seen in these figures, 22, 23 and 24, the solutions obtained with the different noise levels in the Cauchy data are not so far from the solution exact. In addition, the error verifies the following inequality

$$\|ue - u^{\delta}\|_{L^2(\Gamma_0)} \leq \delta$$

This shows that the DRA algorithm is stable because the noise and the error obtained are of the same order. In addition, we note that the oscillations present in the data, see part (a) of Fig. 22, Fig. 23 and Fig. 24, have been absorbed. This proves the regularizing character of our DRA algorithm.

## 6. Conclusion

It was noted from from the numerical discussion that the dynamical relaxation factor has many advantages:

- The algorithm developed is one of the most effective techniques for studying the inverse problems of the Helmholtz equation, capable of ensuring convergence in the case where the wavenumber is large without prior determination of the interval of convergence for the relaxation factor $\theta$.
- It improves the rate of convergence significantly compared to the algorithm with fixed relaxation, especially when the interval of fixed relaxed factor becomes tight.
- The algorithm is very fast and produces a fairly accurate solution regardless of the geometry or regularity of the data.
- The dynamical selection for $\theta^m$ is a successful strategy in order to avoid using any regularization or selection parameter.
- The algorithm presents a strong numerical stability even for data with a very high degree of noise in the Cauchy data.

In conclusion, a dynamic choice of the relaxed alternative algorithm relaxation factor to solve the Cauchy problem associated with the Helmholtz equation proposed in [4] has been developed. This avoids the prior search for an optimal relaxation parameter depending on $k$ to ensure convergence. This also avoids the slowness of this algorithm when the fixed relaxation effect becomes weak. Our algorithm, noted DRA, therefore creates an automicity character which ensures the user a very rapid convergence without any prior intervention on his part. The different numerical results show its superiority over the other iterative or non-dependent methods depending on the search for an optimal parameter.

## Acknowledgement

This work was revised during the visit of Mourad Nachaoui, at the Laboratoire de Mathématiques Jean Leray, Université de Nantes (France), CNRS UMR 6629. This scientific stay was funded by the “Fédéération de Recherche Mathéematiques des Pays de Loire-FR CNRS 2962”.

## REFERENCES


1. S. Andrieux, T. Baranger, and A.B. Abda, *Solving cauchy problems by minimizing an energy-like functional*, Inverse problems 22 (2006), p. 115.
2. S. Avdonin, V. Kozlov, D. Maxwell, and M. Truffer, *Iterative methods for solving a nonlinear boundary inverse problem in glaciology*, J. Inverse Ill-Posed Probl. 17 (2009), pp. 239–258. MR 2527428
3. K. Berdawood, A. Nachaoui, R. Saeed, M. Nachaoui, and F. Aboud, *An efficient dn alternating algorithm for solving an inverse problem for helmholtz equation*, Discrete & Continuous Dynamical Systems-S 15 (2022), p. 57.
4. K.A. Berdawood, A. Nachaoui, M. Nachaoui, and F. Aboud, *An effective relaxed alternating procedure for cauchy problem connected with helmholtz equation*, Numerical Methods for Partial Differential Equations n/a. Available at https://onlinelibrary.wiley.com/doi/abs/10.1002/num.22793.
5. K.A. Berdawood, A. Nachaoui, R. Saeed, M. Nachaoui, and F. Aboud, *An alternating procedure with dynamic relaxation for cauchy problems governed by the modified helmholtz equation*, Advanced Mathematical Models & Applications 5 (2020), pp. 131–139.
6. A. Bergam, A. Chakib, A. Nachaoui, and M. Nachaoui, *Adaptive mesh techniques based on a posteriori error estimates for an inverse cauchy problem*, Applied Mathematics and Computation 346 (2019), pp. 865–878.
7. F. Berntsson, V.A. Kozlov, L. Mpinganzima, and B.O. Turesson, *An alternating iterative procedure for the Cauchy problem for the Helmholtz equation*, Inverse Probl. Sci. Eng. 22 (2014), pp. 45–62. MR 3173606
8. F. Berntsson, V. Kozlov, L. Mpinganzima, and B.O. Turesson, *Robin-Dirichlet algorithms for the Cauchy problem for the Helmholtz equation*, Inverse Probl. Sci. Eng. 26 (2018), pp. 1062–1078. MR 3781581
9. A. Chakib, A. Nachaoui, and M. Nachaoui, *Existence analysis of an optimal shape design problem with non coercive state equation*, Nonlinear Analysis: Real World Applications 28 (2016), pp. 171–183.
10. A. Chakib, A. Nachaoui, M. Nachaoui, and H. Ouaissa, *On a fixed point study of an inverse problem governed by stokes equation*, Inverse Problems 35 (2018), p. 015008.
11. A. Chakib, A. Ellabib, A. Nachaoui, and M. Nachaoui, *A shape optimization formulation of weld pool determination*, Applied Mathematics Letters 25 (2012), pp. 374–379.
12. L. Chang, W. Gong, G. Sun, and N. Yan, *Pde-constrained optimal control approach for the approximation of an inverse cauchy problem*, Inverse Problems and Imaging 9 (2015), pp. 791–814.
13. R. Chapko and B.T. Johansson, *An alternating potential-based approach to the Cauchy problem for the Laplace equation in a planar domain with a cut*, Comput. Methods Appl. Math. 8 (2008), pp. 315–335. MR 2604745
14. J.T. Chen and F. Wong, *Dual formulation of multiple reciprocity method for the acoustic mode of a cavity with a thin partition*, Journal of Sound and Vibration 217 (1998), pp. 75–95.
15. M. Choulli, *Une introduction aux problèmes inverses elliptiques et paraboliques*, Mathématiques & Applications (Berlin) [Mathematics & Applications] Vol. 65, Springer-Verlag, Berlin, 2009. MR 2554831
16. D.L. Colton, R. Kress, and R. Kress, *Inverse acoustic and electromagnetic scattering theory*, Vol. 93, Springer, 1998.
17. R. Dautray and J.L. Lions, *Mathematical Analysis and Numerical Methods for Science and Technology: Volume 2 Functional and Variational Methods*, Vol. 2, Springer Science & Business Media, 1999.
18. T. Delillo, V. Isakov, N. Valdivia, and L. Wang, *The detection of the source of acoustical noise in two dimensions*, SIAM Journal on Applied Mathematics 61 (2001), pp. 2104–2121.
19. T. DeLillo, V. Isakov, N. Valdivia, and L. Wang, *The detection of surface vibrations from interior acoustical pressure*, Inverse Problems 19 (2003), p. 507.
20. A. Ellabib and A. Nachaoui, *An iterative approach to the solution of an inverse problem in linear elasticity*, Math. Comput. Simulation 77 (2008), pp. 189–201. MR 2397893
21. A. Ellabib, A. Nachaoui, and A. Ousaadane, *Mathematical analysis and simulation of fixed point formulation of cauchy problem in linear elasticity*, Mathematics and Computers in Simulation 187 (2021), pp. 231–247.
22. M. Essaouini, A. Nachaoui, and S. El Hajji, *Numerical method for solving a class of nonlinear elliptic inverse problems*, J. Comput. Appl. Math. 162 (2004), pp. 165–181. MR 2043504
23. M. Essaouini, A. Nachaoui, and S. El Hajji, *Reconstruction of boundary data for a class of nonlinear inverse problems*, J. Inverse Ill-Posed Probl. 12 (2004), pp. 369–385. MR 2085380
24. R.B. Fatma, M. Azaez, A.B. Abda, and N. Gmati, *Missing boundary data recovering for the helmholtz problem*, Comptes Rendus Mcanique 335 (2007), pp. 787 – 792.
25. P. Grisvard, *Elliptic problems in nonsmooth domains*, SIAM, 2011.
26. J. Hadamard, *Lectures on Cauchy's problem in linear partial differential equations*, Courier Corporation, 2003.
27. T. Hohage, *Lecture notes on inverse problems* (2002).
28. V. Isakov, *Inverse problems for partial differential equations*, Vol. 127, Springer, 2006.
29. B.T. Johansson and V.A. Kozlov, *An alternating method for Cauchy problems for Helmholtz-type operators in non-homogeneous medium*, IMA J. Appl. Math. 74 (2009), pp. 62–73. MR 2471322
30. B.T. Johansson and L. Marin, *Relaxation of alternating iterative algorithms for the Cauchy problem associated with the modified Helmholtz equation*, CMC Comput. Mater. Continua 13 (2009), pp. 153–189 (2010). MR 2648009
31. M. Jourhmane and A. Nachaoui, *A relaxation algorithm for solving a cauchy problem*, in *on Inverse Problems in Engineering, Engineering*, Proc. of the 2nd Internat. Conf. Vol. 1, Foundation Editor, 1996, pp. 151–158.
32. M. Jourhmane and A. Nachaoui, *An alternating method for an inverse Cauchy problem*, Numer. Algorithms 21 (1999), pp. 247–260. MR 1725728
33. M. Jourhmane and A. Nachaoui, *Convergence of an alternating method to solve the Cauchy problem for Poisson's equation*, Appl. Anal. 81 (2002), pp. 1065–1083. MR 1948031
34. A. Karageorghis, B. Johansson, and D. Lesnic, *The method of fundamental solutions for the identification of a sound-soft obstacle in inverse acoustic scattering*, Applied Numerical Mathematics 62 (2012), pp. 1767–1780.

35. R.V. Kohn and A. McKenney, *Numerical implementation of a variational method for electrical impedance tomography*, Inverse Problems 6 (1990), p. 389.
36. V.A. Kozlov, V.G. Maz'ya, and A.V. Fomin, *An iterative method for solving the Cauchy problem for elliptic equations*, Zh. Vychisl. Mat. i Mat. Fiz. 31 (1991), pp. 64–74. MR 1099360
37. V.A. Kozlov and V.G. Maz'ya, *Iterative procedures for solving ill-posed boundary value problems that preserve the differential equations*, Algebra i Analiz 1 (1989), pp. 144–170.
38. R. Lattes and J. Lions, *Méthode de quasi-réversibilité et applications. dunod, paris, 1967*, English Translation Elsevier, New York (1969).
39. R. Lattes and J. Lions, *Quasi-inversion method and its applications* (1970).
40. R. Lattès and J.L. Lions, *The method of quasi-reversibility: applications to partial differential equations*, Tech. Rep., 1969.
41. M.M. Lavrent'ev, *On the cauchy problem for laplace equation*, Izvestiya Rossiiskoi Akademii Nauk. Seriya Matematicheskaya 20 (1956), pp. 819–842.
42. L. Marin, L. Elliott, P.J. Heggs, D.B. Ingham, D. Lesnic, and X. Wen, *An alternating iterative algorithm for the Cauchy problem associated to the Helmholtz equation*, Comput. Methods Appl. Mech. Engrg. 192 (2003), pp. 709–722. MR 1952356
43. L. Marin, *A relaxation method of an alternating iterative (mfs) algorithm for the Cauchy problem associated with the two-dimensional modified Helmholtz equation*, Numer. Methods Partial Differential Equations 28 (2012), pp. 899–925. MR 2902069
44. L. Marin and B.T. Johansson, *A relaxation method of an alternating iterative algorithm for the Cauchy problem in linear isotropic elasticity*, Comput. Methods Appl. Mech. Engrg. 199 (2010), pp. 3179–3196. MR 2740785
45. A. Nachaoui, M. Nachaoui, A. Chakib, and M. Hilal, *Some novel numerical techniques for an inverse cauchy problem*, Journal of Computational and Applied Mathematics 381 (2021), p. 113030.
46. A. Nachaoui, *An improved implementation of an iterative method in boundary identification problems*, Numer. Algorithms 33 (2003), pp. 381–398. MR 2005577
47. A. Nachaoui, *Numerical linear algebra for reconstruction inverse problems*, Journal of computational and applied mathematics 162 (2004), pp. 147–164.
48. A. Nachaoui, F. Aboud, and M. Nachaoui, *Acceleration of the KMF algorithm convergence to solve the Cauchy problem for Poisson's equation*, in *Mathematical control and numerical applications*, Springer Proc. Math. Stat. Vol. 372, Springer, Cham, [2021] ©2021, pp. 43–57. Available at https://doi.org/10.1007/978-3-030-83442-5_4. MR 4378960
49. A. Nachaoui and H.W. Salih, *An analytical solution for the nonlinear inverse cauchy problem*, Advanced Mathematical Models & Applications 6 (2021), pp. 191–205.
50. M. Nachaoui, A. Nachaoui, and T. Tadumadze, *On the numerical approximation of some inverse problems governed by nonlinear delay differential equation*, RAIRO-Operations Research 56 (2022), pp. 1553–1569.
51. H. Ouaissa, A. Chakib, A. Nachaoui, and M. Nachaoui, *On numerical approaches for solving an inverse cauchy stokes problem*, Applied Mathematics & Optimization 85 (2022), pp. 1–37.
52. S.M. Rasheed, A. Nachaoui, M.F. Hama, and A.K. Jabbar, *Regularized and preconditioned conjugate gradient like-methods methods for polynomial approximation of an inverse cauchy problem*, Advanced Mathematical Models & Applications 6 (2021), pp. 89–105.
53. T. Regińska and K. Regiński, *Approximate solution of a cauchy problem for the helmholtz equation*, Inverse problems 22 (2006), p. 975.
54. J.D. Shea, P. Kosmas, S.C. Hagness, and B.D. Van Veen, *Three-dimensional microwave imaging of realistic numerical breast phantoms via a multiple-frequency inverse scattering technique*, Medical physics 37 (2010), pp. 4210–4226.
55. A.N. Tikhonov, *On the solution of ill-posed problems and the method of regularization*, in *Doklady Akademii Nauk*, Vol. 151. Russian Academy of Sciences, 1963, pp. 501–504.